

Forward and transverse energies in relativistic heavy ion collisions at 14.6 GeV/c per nucleon

(The E-802 Collaboration, Brookhaven National Laboratory)

T. Abbott,^{(4),a} Y. Akiba,⁽⁷⁾ D. Alburger,⁽²⁾ D. Beavis,⁽²⁾ R.R. Betts,⁽¹⁾
 L. Birstein,⁽²⁾ M.A. Bloomer,⁽¹⁰⁾ P.D. Bond,⁽²⁾ C. Chasman,⁽²⁾ Y.Y. Chu,⁽²⁾
 B.A. Cole,⁽¹⁰⁾ J.B. Costales,^{(10),b} H.J. Crawford,⁽³⁾ J.B. Cumming,⁽²⁾
 R. Debbe,⁽²⁾ E. Duek,⁽²⁾ J. Engelage,^(3,9) S.Y. Fung,⁽⁴⁾ L. Grodzins,⁽¹⁰⁾
 S. Gushue,⁽²⁾ H. Hamagaki,⁽⁷⁾ O. Hansen,⁽²⁾ P. Haustein,⁽²⁾ S. Hayashi,⁽⁷⁾
 S. Homma,⁽⁷⁾ H.Z. Huang,^{(10),c} Y. Ikeda,^{(8),d} I. Juricic,^{(3),e} S. Katcoff,⁽²⁾
 S. Kaufman,⁽¹⁾ K. Kimura,⁽⁸⁾ K. Kitamura,^{(6),f} K. Kurita,⁽⁵⁾ R.J. Ledoux,⁽¹⁰⁾
 M.J. LeVine,⁽²⁾ Y. Miake,^(2,11) R.J. Morse,⁽¹⁰⁾ B. Moskowitz,⁽²⁾ S. Nagamiya,⁽⁵⁾
 J. Olness,⁽²⁾ C.G. Parsons,⁽¹⁰⁾ L.P. Remsberg,⁽²⁾ M. Sarabura,^{(10),g} A. Shor,^{(2),h}
 P. Stankus,⁽⁵⁾ S.G. Steadman,⁽¹⁰⁾ G.S.F. Stephans,⁽¹⁰⁾ T. Sugitate,⁽⁶⁾
 M. Tanaka,⁽²⁾ M.J. Tannenbaum,⁽²⁾ M. Torikoshi,^{(7),i} J.H. van Dijk,⁽²⁾
 F. Videbaek,⁽²⁾ M. Vient,^{(4),j} P. Vincent,^{(2),k} E. Vulgaris,^{(10),l} V. Vutsadakis,⁽¹⁰⁾
 W.A. Watson III,^{(2),m} H.E. Wegner,⁽²⁾ D.S. Woodruff,⁽¹⁰⁾ Y.D. Wu,⁽⁵⁾ and
 W.A. Zajc⁽⁵⁾

⁽¹⁾ Argonne National Laboratory, Physics Division, Argonne, Illinois 60439

⁽²⁾ Brookhaven National Laboratory, Upton, New York 11973

⁽³⁾ University of California, Space Sciences Laboratory, Berkeley, California 94720

⁽⁴⁾ University of California, Riverside, California 92507

⁽⁵⁾ Columbia University, New York, New York 10027

and Nevis Laboratories, Irvington, New York 10533

⁽⁶⁾ Hiroshima University, Hiroshima 730, Japan

⁽⁷⁾ Institute for Nuclear Study, University of Tokyo, Tokyo 188, Japan

⁽⁸⁾ Kyushu University, Fukuoka 812, Japan

⁽⁹⁾ Lawrence Livermore National Laboratory, Livermore, California 94550

⁽¹⁰⁾ Massachusetts Institute of Technology, Laboratory for Nuclear Science, Cambridge, Massachusetts 02139

⁽¹¹⁾ University of Tokyo, Department of Physics, Tokyo 113, Japan

(Received 7 May 1991)

Forward and transverse energy spectra and the correlation between these two global variables have been measured for the interaction of 14.6A GeV/c ²⁸Si ions with ²⁷Al and ¹⁹⁷Au. The energy in produced particles near midrapidity is observed to be negatively correlated with forward energy. There is minimal target mass dependence of this correlation for peripheral and semicentral interactions (forward energies > 80 GeV). However, the fact that transverse energies for more central collisions in Au become increasingly larger than those in Al (~ 50% greater in the limit of zero forward energy) provides evidence for multiple interactions of projectile nucleons in the larger target. The experimental results are discussed in terms of calculations based on a model for nucleus-nucleus interactions.

I. INTRODUCTION

Interest in the interaction of relativistic heavy ions with nuclei has been enhanced by the possibility that a quark-gluon plasma (QGP) might be formed at the high densities and temperatures created in such reactions. Experiment 802 (E802) at the Brookhaven Tandem Alternating Gradient Synchrotron (AGS) Complex is one of a series of experiments at Brookhaven National Laboratory (BNL) and CERN which are examining high-energy nucleus-nucleus collisions for possible evidence of QGP formation or other new processes [1]. A general description of the E802 experimental setup and results on particle production at midrapidities obtained with its large

magnetic spectrometer are given elsewhere [2,3].

The present work examines the flow of energy from the beam (forward energy) into the "midrapidity" region (transverse energy) based on measurements with the E802 Zero Degree Calorimeter, ZCAL, and the Lead Glass Array, PbGL. The interpretation of such measurements rests on two assumptions: (1) that forward energy is a measure of the number of projectile spectator nucleons which can be related to the impact parameter, and (2) that the efficiency for conversion of energy originally carried by the projectile participants into energy in the form of produced particles can be inferred from transverse energy production. Calculations based on the Fritiof model [4] provide a framework for the interpreta-

tion of the experimental results.

We are particularly interested in events where a large fraction of the projectile energy is radiated into midrapidity, away from the projectile and target fragmentation regions. The target mass dependence of transverse energy production for such central events at this bombarding energy has been interpreted as indicating “projectile stopping” in nuclei heavier than Cu [5–7]. This term is an operational definition of the observation that maximum transverse energy increases much less rapidly than does target thickness in a sequence such as Cu, Ag, and Au. The implication is that when a projectile traverses the diameter of a heavy nucleus, the potential for particle production is exhausted in early collisions. Experimental rapidity distributions [3] indicate that this stopping is not consistent with an amalgamation of projectile and swept-out target nucleons to form a slowly-moving equilibrated fireball.

II. EXPERIMENTAL

A. Beam and interaction trigger

The 14.6A GeV/ c ^{28}Si beam had a diameter of ~ 4 mm (averaged over the beam spill) and a purity of $> 99\%$ at the E802 target position. ^{28}Si ions were selected by requiring $Z = 14$ signals from two scintillators before the target. Beam halo was suppressed by an upstream “hole” scintillation veto counter. The beam intensity was typically $(3\text{--}5)\times 10^4$ particles during a spill of ~ 600 msec. A minimum-bias trigger (INT) was built by requiring that a particle that had the beam charge before the target did not appear in the $Z = 14$ peak in a scintillation “bullseye” counter located 1.1 m in front of the forward calorimeter, ZCAL, which was 11.7 m downstream of the target. For typical settings of the bullseye discriminator, 87% of events with $Z = 13$ fragments and 17% of those with $Z = 12$ fragments are also rejected.

B. Lead glass

The Lead Glass Array of E802 is composed of 245 14.5×14.5 -cm square-faced SF5 blocks. They are stacked with their front faces 3.0 m downstream of the target in a configuration providing approximately half azimuthal coverage over laboratory polar angles from 8.5° to 32° ($1.25 < \eta_{\text{lab}} < 2.60$ in pseudorapidity). The laboratory rapidity of the nucleon-nucleon center of mass, $y_{\text{c.m.}}^{NN}$, is 1.72 at this energy. Two signals available from the PbGl array on an event-by-event basis are total energy $E_{\text{tot}}^{\text{PbGl}}$, equal to $\sum E_i$, and transverse energy E_T^{PbGl} , equal to $\sum E_i \sin \theta_i$, where E_i and θ_i are the energies and center angles of the individual blocks, respectively. Sums include only those blocks showing a signal ≥ 0.05 GeV. The transverse energy signal is emphasized in the present work as a measure of the conversion of projectile energy into produced particles [8]. A central collision trigger (PB2) was derived from a high-threshold discriminator on the E_T^{PbGl} analog signal that was set to accept a non-

inal few percent of the minimum-bias (INT) events. Because under normal running conditions only a small sample of the INT events are recorded, this PB2 trigger is useful for increasing statistics on the high-energy tails of the spectra.

Although a lead glass signal is commonly considered to be a measure of “neutral energy” from the decay of π^0 and η^0 mesons, charged hadrons will also contribute due to their Čerenkov radiation. Relativistic charged pions directly incident on the PbGl array were observed to give an equivalent energy of ~ 0.45 GeV per particle [9]. Calculations described in the Appendix indicate that charged and neutral particles make approximately equal contributions to the energy observed in the present configuration [10]. This confirms a previous estimate for this detector [5]. No attempt was made to separate the components since the response of the PbGl array to Čerenkov light is linear to $< 1\%$ whatever the source. The absolute energy scale for the array was set by calibration in an electron beam. Early results for ^{16}O interactions from a prototype PbGl array that provided 2π azimuthal coverage and for ^{28}Si interactions in the present configuration have been published [5,6].

C. The zero degree calorimeter, ZCAL

ZCAL is an Fe/scintillator calorimeter generally patterned after the ZDC calorimeter of WA80 [11] at CERN. Major differences are the use of iron as the stopping medium in place of uranium and a novel segmentation. ZCAL has a cross-sectional area of 60×60 cm 2 . Its fundamental stacking unit consists of a 1-cm iron plate followed by a 0.3-cm scintillator. It is longitudinally segmented into two sections: the first, H $_1$, contains 32 stacking units (20.4 radiation lengths or 2.0 interaction lengths λ); the second, H $_2$, has 106 stacking units or 6.7 λ . Light is collected from each section of ZCAL by eight wavelength shifter bars (two per side) and brought to photomultiplier tubes at the rear of the calorimeter by light guides. The calorimeter was calibrated using primary ^{16}O and ^{28}Si beams as well as projectile fragments [12]. After pedestal subtraction, gains of the 16 phototubes were adjusted and the signals added, weighting those from H $_1$ and those from H $_2$ in the ratio 57:43. This weighting gives an optimized resolution (σ/E) of 3.6% for 381-GeV ^{28}Si ions. There is good proportionality between light output and projectile mass for ^1H to ^{28}Si at 14.6A GeV/ c with a root-mean-square deviation of ~ 0.8 GeV over this range. The 30-cm half of ZCAL’s face subtends a polar angle of 25.6 mrad at the target, which corresponds to $\eta = 4.4$ or a perpendicular momentum transfer of 375 MeV/ c per nucleon to a particle of beam rapidity. Additional details on ZCAL are available elsewhere [12].

III. EXPERIMENTAL RESULTS AND DISCUSSION

A. Forward and transverse energy spectra

Minimum-bias histograms (INT trigger) of forward and transverse energies obtained with ZCAL and the

PbGl array for 817-mg/cm² Al and 944-mg/cm² Au targets (3% and 1% of an interaction length for ²⁸Si, respectively) are shown in Fig. 1. These results have been corrected for target-out contributions which were measured to be the equivalent of an $\sim 0.5\%$ target. The corrections had a large effect on ZCAL spectra in the vicinity of the beam energy; however, their effect below ~ 340 GeV is minimal. Target-out corrections to the PbGl spectra are significant only below ~ 1 GeV. For the discriminator setting used in the present work, the corrected INT cross sections are 1.3 ± 0.1 b for Al and 3.6 ± 0.2 b for Au. Errors include both statistical uncertainties and estimates of systematic effects due to the relatively large target-out corrections. The experimental configuration for the measurements depicted as histograms was such that particles emitted at angles > 7 mrad passed through beam pipe, flanges, etc. Trajectories between 7 and 14 mrad experienced on the average 1.3 nucleon interaction lengths. The filled points in Fig. 1 were obtained with a larger diameter beam pipe that had a 14-mrad unobscured opening and an average of only 0.8 interaction lengths out to the full acceptance of ZCAL. Changes, if any, in going to the more open configuration are small, demonstrating that ZCAL spectra are not sensitive to collimation effects.

Regions of the spectra defined by the ‘‘central’’ PB2 trigger are shaded in Fig. 1. These include 1.4% of the events for Al and 2.1% for Au. The PB2 data establish that the highest transverse energy events are associated with low-energy deposition in ZCAL for both targets. The most significant difference between the results for Al and Au, aside from the $\sim 50\%$ increase in transverse energy with target size, is the behavior of the ZCAL spectra at low energies. While the intensity drops by a factor of ~ 30 below 80 GeV for Al, it rises to a peak at or near zero energy for Au. The shaded distribution for the PB2 trigger indicates that the most probable result of a central Si + Au collision is that no projectile spectators remain within the calorimeter acceptance when transverse energy is a maximum. The projectile is effectively stopped. The mean ZCAL energy associated with the PB2 events for Au is 11.8 GeV. This value sets an upper limit on the energy in produced particles and interacting projectile nucleons from a central Si + Au interaction which reach ZCAL. The spectrum from ZCAL for Al selected by the PB2 trigger gives clear evidence that the smaller nucleus is not able to completely stop a Si projectile. Some nucleons in the nuclear edge region do not interact even in the most central events. The peak in the PB2 triggered distribution for Al corresponds to ~ 4 projectile nucleons remaining within ZCAL’s acceptance. At least some part of ZCAL’s behavior at low energies is a consequence of nuclear geometry. Total overlap for Si + Al can only occur at zero impact parameter for which the cross section is zero. In contrast, there is a range of impact parameters for complete overlap in Si + Au interactions, hence, a significant cross section for events with low E_{ZCAL} . Realistic nuclear geometries are incorporated in the models discussed in Section IIIC and the Appendix. Additional details of ZCAL’s response may also be found there.

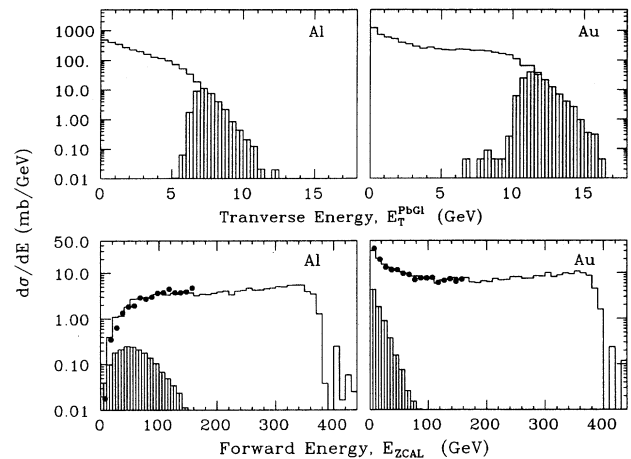


FIG. 1. Transverse and forward energy spectra from the interaction of $14.6A$ GeV/c ²⁸Si with aluminum and gold. Experimental data from the lead glass array PbGl and the downstream calorimeter ZCAL of E802 are shown as histograms. Spectral regions selected by the central PB2 trigger are shaded. Corrections for target out have been applied. Target thicknesses were 3% and 1% of a ²⁸Si interaction length for Al and Au, respectively. Filled points on the ZCAL spectra at low energies were obtained with a less restrictive beam pipe configuration. They are included to show that the spectra are not sensitive to collimation effects, see text.

B. Correlation between forward and transverse energy

ZCAL energy should vary, to a first approximation, linearly with the number of projectile spectators or participants, n_{ps} or n_{pp} , respectively: $E_{ZCAL} \approx 13.6n_{ps}$ or $E_{ZCAL} \approx 13.6(28 - n_{pp})$. Transverse energy is expected to increase with n_{pp} and should therefore be negatively correlated with forward energy. This has been demonstrated by results for ¹⁶O+Au interactions at higher energies [13,14] that confirm the intuitive notion that central collisions exhibit small forward energies and large transverse energies and vice versa. The present data shown in Fig.1 provide evidence for the negative correlation at $14.6A$ GeV/c.

The PbGl-ZCAL correlation is examined in more detail in Fig. 2. The upper portion of this figure shows 20-GeV-wide slices through the correlation surfaces for the two targets, centered at E_{ZCAL} values of 10, 110, 230, and 350 GeV. The distribution of transverse energy associated with a particular E_{ZCAL} is approximately Gaussian (or the tail of a Gaussian in the case of high E_{ZCAL}). For very peripheral reactions ($E_{ZCAL} > 300$ GeV) the most probable transverse energy is zero. As the ZCAL energy decreases, the peak position moves out from zero. Distributions for $E_{ZCAL} = 110$ GeV in Fig. 2 are cleanly separated from the origin, and the probability for low transverse energy becomes vanishingly small in central and semicentral events. At E_{ZCAL} values where the distributions are separated from the origin, the most prob-

able PbGl energy is essentially equal to the mean.

A striking feature of the correlation surface is that there is a negligible dependence on target mass for interactions involving less than about half of the projectile nucleons. This is apparent in the lower part of Fig. 2 which shows the dependence of the mean E_T^{PbGl} on E_{ZCAL} . The target mass dependence remains weak even down to $E_{\text{ZCAL}} \sim 80$ GeV. Such behavior is consistent with transverse energy production in peripheral interactions by a series of independent projectile-nucleon, target-nucleon single collisions. Each such collision will produce the same distribution of E_T^{PbGl} which implies a linear and target independent relationship, consistent with the data in the peripheral region.

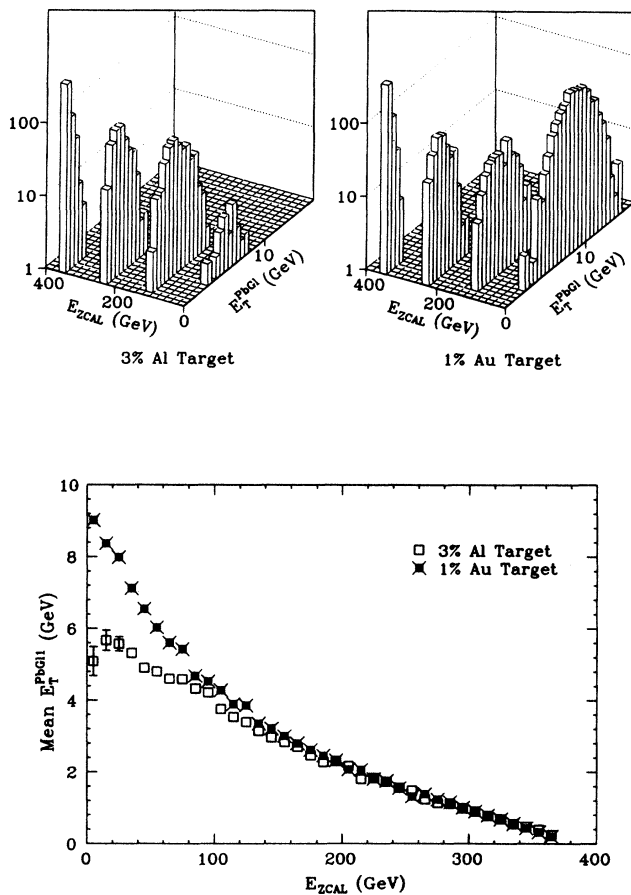


FIG. 2. Some aspects of the negative correlation between transverse energy (E_T^{PbGl}) and forward energy (E_{ZCAL}) in the interactions of $14.6A$ GeV/ c ^{28}Si with Al and Au. The two upper panels show slices through the correlation surfaces revealing the nearly Gaussian shapes of the E_T^{PbGl} spectra for fixed E_{ZCAL} . The lower panel shows the dependence of the mean E_T^{PbGl} on E_{ZCAL} . A characteristic feature of these data is the target independence for peripheral events, i.e., those with $E_{\text{ZCAL}} > 190$ GeV.

A pronounced target dependence and a nonlinearity develop when E_{ZCAL} drops below ~ 80 GeV, into the region of central collisions. This suggests a contribution from multiple collisions in the additional target matter provided by the larger nucleus. As was discussed in connection with Fig. 1, the probability for complete energy removal from the beam becomes small in the case of an Al target, but rises to a peak for Au. The present data indicate that the mean transverse energy associated with such complete energy removal events is $\sim 50\%$ larger for Au than for Al. For the lowest energy slice in Fig. 2 ($E_{\text{ZCAL}} = 0 - 20$ GeV), the highest transverse energies for the Al target fall below the mean of the distribution for Au. These results suggest that beam participants that are thrown out of ZCAL's acceptance in their initial interactions, their collision partners, and/or particles produced in the initial collisions have the potential for generating additional transverse energy in the larger target. Any effect due to a change in the acceptance of the PbGl as a consequence of a change in the pseudorapidity distribution of produced particles is $\sim 10\%$, as discussed in the Appendix.

C. Comparison with model calculations

Model calculations can provide a useful framework for the discussion of experimental data. The model adopted for the present work is based on the Lund Monte Carlo event generator FRITIOF [4] coupled to a program that imposed the INT selection on the events and simulated the response characteristics of ZCAL (including its resolution) and the PbGl array in a simplified way. FRITIOF treats a nucleus-nucleus interaction as a series of nucleon-nucleon collisions in the appropriate nuclear geometry. Although a given projectile or target nucleon can be involved in multiple binary encounters, hadronization of the strings takes place only after all interactions are completed, hence no cascading is considered. In addition to Al and Au, the targets studied experimentally, calculations were also performed for Cu and Ag to examine further the development of trends with target mass. Details of these calculations are given in the Appendix. Agreement at the $\sim 10\%$ level between the predicted INT cross sections, 1.2 b for Al and 3.2 b for Au and those measured, 1.3 ± 0.1 and 3.6 ± 0.2 , respectively, is reasonable considering the uncertainties in the target-out correction in the experiment and the definition of the INT trigger in the calculation.

Calculated forward energy (ZCAL) and transverse energy (PbGl) spectra for the four targets are shown as smooth curves in Fig. 3. The experimental results for Al and Au are superimposed as filled points. The model qualitatively predicts an evolution of the ZCAL spectra with increasing target size similar to that observed. The minimum at $E_{\text{ZCAL}} \sim 0$ for Al in the calculations fills in for heavier elements, becoming a peak for Au. However, there is a significant quantitative difference. Model cross sections are systematically shifted from low ZCAL

energy to high ZCAL energy (from central to more peripheral interactions) when compared to the experimental data. This is particularly apparent in the case of Si + Al where the actual falloff occurs at lower energies and is less rapid than that predicted. The calculated cross section at $E_{ZCAL} = 20$ GeV is about an order of magnitude lower than observed.

Because ZCAL energy is determined primarily by the number of projectile spectator nucleons reaching the calorimeter (see the Appendix), the difference in spectral shape reflects an intrinsic underprediction of central events by FRITIOF and/or a problem in the treatment of spectator nucleons by the subsequent calculation. FRITIOF simply counts the spectator nucleons. It gives no information on their angular distribution or state of aggregation. Angular distributions [15,16] of projectile fragments with $Z \geq 2$, i.e., $\geq {}^3\text{He}$, ${}^4\text{He}$, are such that they will all impact near the center of the calorimeter and contribute 13.6 GeV/nucleon to the ZCAL energy in agreement with the assumption of the present calculation. Cases with one or two spectators were assumed to have a broader angular distribution [15] and be subject to losses in the edge region of ZCAL. There is evidence that many events involve multiple fragments and/or nucleons (multifragmentation). To the extent that nucleons or light particles from multifragmentation events miss ZCAL or impinge in the edge region where leakage occurs, the prediction would be moved to lower energies in better agreement with the experiment. For example, only 36% of the charge-changing cross section in Si + Al interactions is observed [17] to lead to fragments with $Z \geq 7$, while FRITIOF predicts that 80% of that cross section is associated with events having ≥ 7 spectator protons.

An interesting test of the model is a comparison of the ZCAL spectrum calculated for central Si+Au interactions, i.e., those involving all 28 projectile nucleons, with the experimental spectrum obtained in coincidence with $E_T^{\text{PbGl}} \geq 12$ GeV. This PbGl energy cut defines a better experimental central trigger that retains approximately

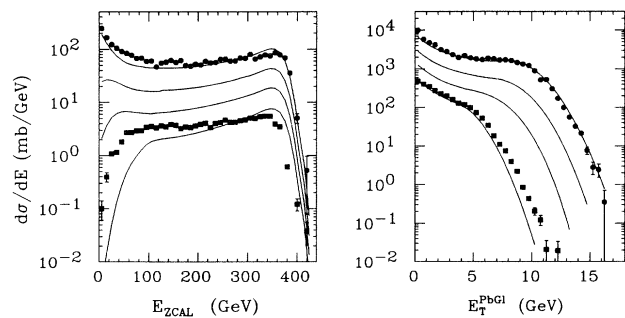


FIG. 3. Comparison of experimental ZCAL and PbGl spectra (filled points) with the results of model calculations (smooth curves). Calculations are for $14.6A$ GeV/c ${}^{28}\text{Si}$ interactions with Al, Cu, Ag, and Au in ascending order. They are displaced upwards by successive factors of 2 for display purposes. Experimental data are shown as points.

one-third of the PB2 events from Au but essentially none of those from Al. For such central Si + Au events, there are no projectile spectators, and the ZCAL energy is determined by produced particles and participant nucleons. Both spectra in Fig. 4 have similar shapes with peaks slightly above zero energy. The experimental mean energy is 10.0 GeV, that calculated, 9.2 GeV. Because the calculation is sensitive to assumptions about leakage in the edge regions of ZCAL, this agreement serves to validate the model, at least in the case of central Si + Au interactions where there are no spectators. Had leakage not been included, the calculated spectrum would have been shifted upwards by $\sim 40\%$.

As can be seen in Fig. 3, the model predicts shapes of the transverse energy (PbGl) spectra very well. There is a good match to the experimental data for Au over the whole range of energies. The predicted magnitude of E_T^{PbGl} for Al is $\sim 10\%$ less than that observed. Although the absolute energy scale of the data in the figure may be uncertain by the order of a few percent, the relative scale for the two targets should be reliable to $\sim 1\%$.

PbGl-ZCAL correlations predicted by the FRITIOF model are compared with the experimental results in Fig. 5. Although the calculation reproduces the general trend of the data for the upper half of the ZCAL energy range, it predicts mean transverse energies the order of 50% too large. The discrepancy decreases with decreasing E_{ZCAL} to $\sim 10\%$ for the most central collisions. In view of the comparisons in Fig. 3, we believe that a major part of these discrepancies may be related to the problems in treating projectile spectators when calculating ZCAL spectra. For a given class of events, say those with 14 spectator nucleons, the calculated mean E_T^{PbGl} (which may be correct for those events) is plotted at too high a ZCAL energy, hence it appears high when compared to

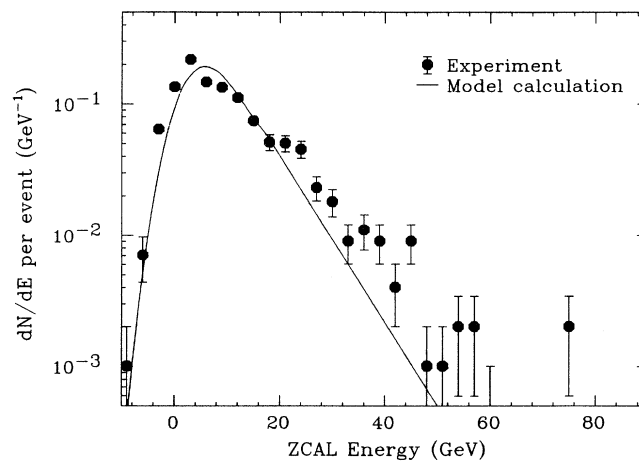


FIG. 4. Comparison of experimental and calculated ZCAL spectra for central Si + Au interactions at $14.6A$ GeV/c. Filled points define the spectrum observed in coincidence with PbGl transverse energies ≥ 12 GeV. The smooth curve is the spectrum calculated for events in which all projectile nucleons interact.

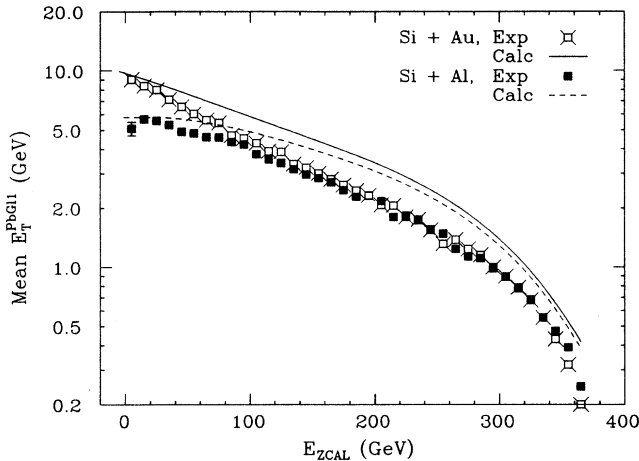


FIG. 5. Comparison of experimental and calculated correlations between mean transverse energy (E_T^{PbGl}) and forward energy ($E_{Z\text{CAL}}$) for 14.6A GeV/c ^{28}Si interactions with Al and Au. Experimental results are shown as points. Results from a calculation based on the FRITIOF model are shown as smooth curves.

experiment in Fig. 2. If this is indeed the case, the model might do better in predicting relative energies.

The experimental target effect as defined by the ratio $E_T^{\text{PbGl}}(\text{Au})/E_T^{\text{PbGl}}(\text{Al})$ is shown in Fig. 6(a) as a function of $E_{Z\text{CAL}}$. Mean transverse energy is essentially independent of target for peripheral reactions. The influence of the larger target appears only in the lower half of the ZCAL range where the ratio rises significantly above unity. Note that uncertainties in the absolute E_T^{PbGl} scale cancel in such a ratio plot.

Target effects inferred from two simpler models are shown in Fig. 6(b). The standard wounded nucleon model (WNM) [18] calculates the number of interacting target and projectile nucleons from realistic nuclear density distributions and an average nucleon-nucleon cross section. Transverse energy is taken to be proportional to the total number of wounded nucleons (projectile + target) and all interacting projectile nucleons are assumed to be thrown out of ZCAL's acceptance. The filled points in Fig. 6(b) indicate that the WNM overpredicts the experimental target dependence.

In contrast to the WNM, the wounded projectile nucleon model (WPNM) considers that transverse energy is dependent only on the number of wounded projectile nucleons. This assumption is suggested by the successful analysis of transverse energy spectra from nucleus-nucleus collisions in terms of n -fold convolutions of experimental $p + A$ spectra [5,19,20], e.g., the $^{16}\text{O} + \text{Au}$ spectrum as a 16-fold convolution of the spectrum from central $p + \text{Au}$ interactions. In the WPNM, a given number of wounded projectile nucleons make the same contribution to transverse energy independent of the target. The open points in Fig. 6(b) indicate the expected absence of a target effect, in clear disagreement with experimental results from the ZCAL-PbGl correlation for

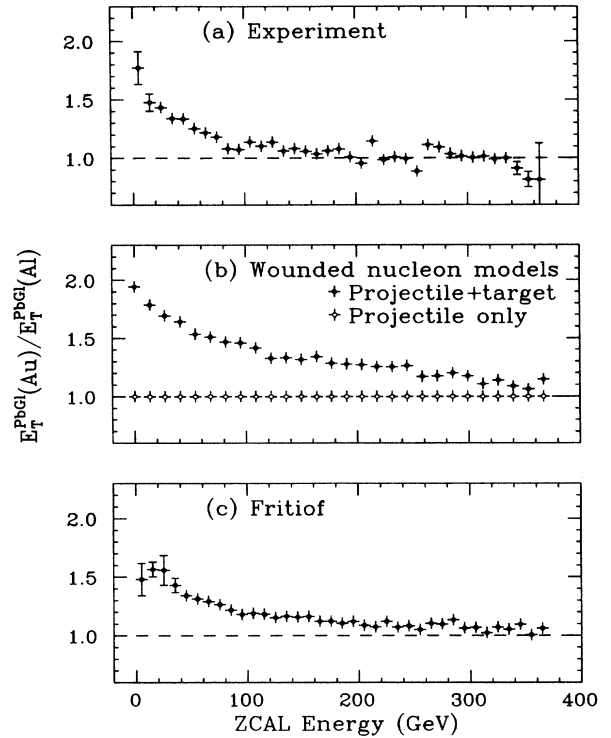


FIG. 6. Target dependence of mean transverse energy for 14.6A GeV/c ^{28}Si interactions with Au and Al. (a) The experimental ratio $E_T^{\text{PbGl}}(\text{Au})/E_T^{\text{PbGl}}(\text{Al})$ as a function of $E_{Z\text{CAL}}$. (b) Ratios predicted by two simple models based on counting wounded nucleons, see text. (c) The ratio predicted by a calculation based on the FRITIOF model.

$E_{Z\text{CAL}} \leq 80$ GeV.

The FRITIOF model [Fig. 6(c)] predicts a target effect intermediate between those of the WNM and WPNM. FRITIOF generally reproduces the experimental target dependence but it is systematically high over the entire ZCAL range by $\sim 10\%$, a shift consistent with the difference between experimental and calculated transverse energy spectra seen in Fig. 3. Since the number distribution of wounded nucleons is similar in FRITIOF and the WNM, the weaker target effect predicted by FRITIOF appears to be related to the treatment of multiple collisions. Initial projectile-nucleon-target-nucleon collisions are at the full beam energy in both models, but subsequent interactions in the FRITIOF model are at appropriately reduced energies, hence the pion multiplicity and the contribution to transverse energy is reduced. In contrast, all wounded nucleons are weighted equally in the WNM and an overprediction of the target dependence of transverse energy is expected for central events in larger nuclei where there are many multiple collisions.

IV. SUMMARY AND CONCLUSIONS

The present work has examined some global features of heavy-ion interactions at 14.6A GeV/c with particular emphasis on the conversion of beam energy into pions

radiated into the midrapidity region. This conversion is observed as a negative correlation between transverse and forward energy for both Si + Al and Si + Au interactions. The highest transverse energy events in the case of Au are shown to be associated with complete loss of forward energy, which can be interpreted as projectile stopping. The Al nucleus is not able to stop a ^{28}Si projectile. Even at zero impact parameter, there is some transparency in the nuclear surface regions. Forward energy equivalent to several nucleons on the average remains even in the most central, highest transverse energy events. Interesting features of the data are the observed lack of target dependence for transverse-energy production in peripheral interactions, indicative of independent single collisions, and that transverse energies for more central collisions in Au become increasingly larger than those in Al ($\sim 50\%$ greater in the limit of zero forward energy), which is evidence for multiple interactions of projectile nucleons in the larger target.

A model for calculating forward and transverse energies based on the FRITIOF event generator is shown to reproduce general trends of the experiment. Despite quantitative problems in predicting ZCAL spectra, the model predicts, in agreement with the data, a shift of only $\sim 50\%$ of the upper edge of the transverse-energy spectra in going from Al to Au, despite a 140% increase in number of nucleon-nucleon collisions (or the equivalent 80% increase in number of participants) in central Si + Au interactions compared to Si + Al. Subsequent collisions after the first at 14.6 GeV/c are much less effective for pion production. In this sense "projectile stopping" is a natural consequence of the low energy/nucleon at the AGS. A similar conclusion can be reached from the observation that the multiplicity of shower particles observed in emulsion studies of $p + A$ collisions at this energy is only slightly greater than that in $p + p$ interactions [21]. Evidence for a reduced contribution from subsequent collisions is also seen in studies of $p + A$ interactions with the E802 spectrometer [22]. Yields integrated over the range $0.6 \leq y \leq 2.6$ were observed to be only $8 \pm 3\%$ larger for π^+ , and only $27 \pm 5\%$ larger for π^- from a Au target compared to Be, despite a threefold increase in the linear dimensions of the targets.

It is clear from the present experiment that global measurements can provide valuable information for event classification and reaction dynamics in relativistic heavy-ion collisions, including the estimation of impact parameters and the effect of multiple collisions. Such data also serve as constraints on any model that may be proposed to explain specific details of these reactions.

ACKNOWLEDGMENTS

We wish to thank the AGS and Tandem operations staffs for providing the excellent ^{28}Si beam. This work was supported by the U.S. Department of Energy under contracts with ANL (W-31-109-ENG-38), BNL (DE-AC02-76CH00016), Columbia University (DE-FG02-86-ER40281), LLNL (W-7405-ENG-48), MIT (DE-AC02-76ER03069), UC Riverside (DE-FG03-86ER40271), and

by NASA under contract with the University of California (NGR-05-003-513), and by the U.S.-Japan High Energy Physics Collaboration Treaty. S. Hayashi would like to acknowledge the Japan Society for the Promotion of Science for financial support.

APPENDIX: FRITIOF MODEL CALCULATIONS

The Lund Monte Carlo code FRITIOF [4] treats a nucleus-nucleus interaction as a series of binary nucleon-nucleon encounters in the appropriate nuclear geometry. A given collision may excite either or both participants, and an excited participant may be further excited in subsequent collisions. For nucleus-nucleus interactions, collisions may also occur between two excited nucleons. Hadronization of the excited objects produced is treated as effectively occurring outside either nucleus, i.e., no cascading of produced particles is considered. Output includes energy, angle, and type of each participant or produced particle resulting from an interaction. Events generated by FRITIOF [23] for Si + Al, Cu, Ag, and Au were input to a program that imposed cuts appropriate for the minimum-bias INT trigger and simulated detection properties of ZCAL and the PbGl array. FRITIOF predicts nuclear reaction cross sections of 1.6, 2.2, 2.8, and 3.8 b for Si interactions with Al, Cu, Ag, and Au, respectively.

The INT trigger used to identify interactions introduces a bias on the experimental data. Projectile fragments with $Z = 14$ are not distinguished from beam particles, and for typical settings of the discriminator on the downstream bullseye scintillator, $\sim 87\%$ of the $Z = 13$ fragments and $\sim 17\%$ of the $Z = 12$ fragments are also rejected. FRITIOF provides no information as to the state of aggregation of the projectile spectator nucleons. However, experimental charge-changing cross sections [17] are substantially lower than those from FRITIOF for the same number of spectator protons. For example, FRITIOF gives 574 mb of cross section for events with 13 spectator protons from Si + Au interactions while the measured cross section for $Z = 13$ fragments is only 180 mb. Based on a parametrization of the measured charge-changing cross sections, the INT cut was imposed only on that fraction of the FRITIOF events with 12 and 13 spectator protons that would have true $Z = 12$ or 13 fragments downstream. This cut has a significant effect in reducing peripheral events contributing to the high-energy end of the ZCAL spectra and to the low energy end of the PbGl spectra. That the INT cross sections calculated in this way, 1.2 b for Al and 3.2 b for Au, are $\sim 10\%$ lower than those measured probably is a consequence of uncertainties in the definition of the INT trigger in the calculation and in the experimental target-out correction.

ZCAL was treated as intercepting a cone of 25-mrad half angle with no leakage of energy for particles impinging at ≤ 10 mrad. Calculations using a program [24] that traced energy deposition in the beam pipe and ZCAL indicate energy loss for particles incident at larger angles which could be approximated as an exponential falloff of

response starting from 1.0 at an angle of 10 mrad and declining to 0.4 at 25 mrad. All calculated ZCAL spectra have been corrected for the experimental resolution which is a quadrature combination of 2.3 GeV of noise with an intrinsic $0.73\sqrt{E}(\text{GeV})$.

There are three contributions to the ZCAL energy; projectile spectator nucleons, participant nucleons (spectator and target), and produced particles. FRITIOF predicts that the shapes of ZCAL spectra primarily reflect the number distribution of projectile spectators. In particular, the peak near zero energy for Au reflects a large cross section, 366 mb, for the interaction of all 28 projectile nucleons. A very low cross section, 0.3 mb, is responsible for the deep valley in the case of Al. Since FRITIOF gives only the number of projectile spectators, there is a problem in how to treat their angular distribution at ZCAL. Experimental data [15,16] indicate that all projectile fragments $\geq {}^3\text{He}$ will fall within the 10 mrad cone where leakage is not expected. However, scaling the $Z = 2$ data of Adamovich *et al.* [16] to nucleons suggests that $\sim 10\%$ of the nucleons will be at larger angles. Based on these data it was assumed that nucleons from events involving one and two projectile spectators are Gaussian distributed in angle with a standard deviation of 6 mrad. With these assumptions, the overall effect of leakage on the contribution of projectile fragments to ZCAL energy is small.

The second and third components of the ZCAL energy define a "participant energy," i.e., participant nucleons + produced particles. Calculated participant energy is plotted as a function of number of projectile spectator nucleons for Al and Au targets in Fig. 7. An analysis of the calculation shows that this participant energy is dominated by projectile participants and that their angular distribution peaks in the vicinity of the edge of ZCAL. As a consequence, leakage or complete loss is significant. Mean participant energies are $\sim 40\%$ lower than those that would be obtained in the absence of leakage. An important feature of Fig. 7 is the attenuation of the participant energy reaching ZCAL by additional interactions in central collisions in the thicker Au nucleus. For events in which all 28 projectile nucleons interact, the mean number of nucleon-nucleon collisions is 66 for Si + Au compared with 28 for Si + Al. The extra 1.4 collisions per projectile nucleon in Au are effective in scattering participants out of ZCAL's acceptance.

Individual PbGl blocks were idealized in this calculation as 15×15 -cm squares centered at the actual block face positions; however, the geometry defining plane was taken to be 15 cm behind the faces. For each particle in an event, block energy was incremented by the actual energy in the case of an incident gamma ray or by 0.45 GeV if struck by a charged particle having $\beta \geq 0.8$ [25]. PbGl total energy for the event was obtained by summing over all blocks having ≥ 0.05 GeV to match the experimental software discriminators. Energies were reduced by $0.934 = (14.5/15)^2$ as an approximate correction for the 0.5-cm dead space between blocks. PbGl transverse energy was a similar sum but weighted by $\sin \theta$ at the block centers. The contribution of gammas, charged pions, pro-

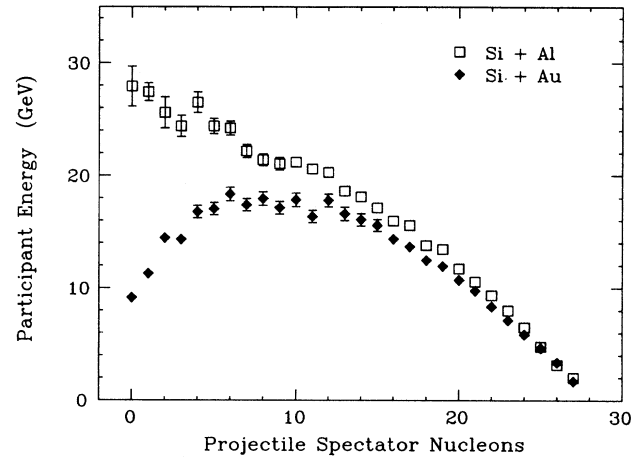


FIG. 7. Calculated mean energy of participant nucleons and produced particles ("participant energy") detected by ZCAL as a function of number spectator nucleons for Si + Al and Si + Au interactions as indicated.

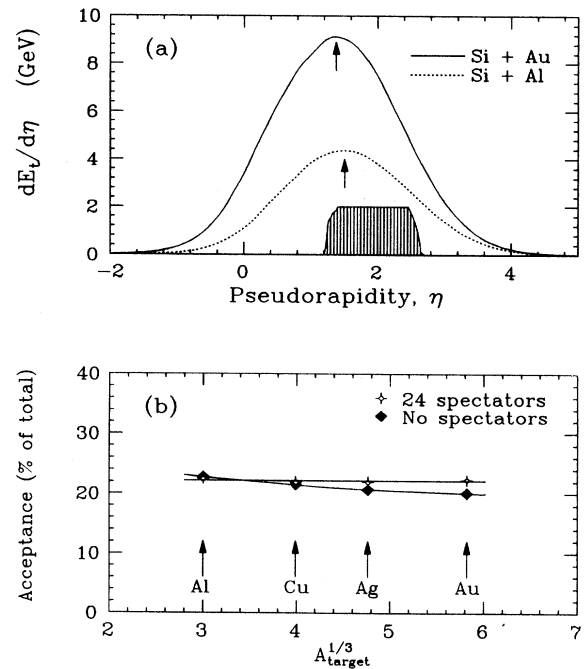


FIG. 8. Calculated properties of the lead glass array of E802. (a) Pseudorapidity distributions of transverse energy for Si + Al and Si + Au interactions. The relative azimuthal coverage of the PbGl array is shown by the shaded histogram. (b) Dependence of PbGl transverse acceptance on target size for typical peripheral interactions (24 spectators) and central collisions (no spectators). Acceptance is defined as the ratio of the observed energy to that which would be observed in a device with the same detection properties but having 4π coverage.

tons, and kaons to the transverse energy was found to vary from 56.6, 36.9, 5.0, and 1.5 %, respectively, for the Al target to 54.6, 37.2, 6.9, and 1.3 % in the case of Au. The FRITIOF model confirms that the PbGl array primarily measures energy in produced particles ($\sim 94\%$) and that $> 50\%$ of the energy is “neutral.”

Other quantities of interest for the interpretation of PbGl spectra can also be obtained from the model. Approximately Gaussian distributions of PbGl transverse energy as a function of pseudorapidity η are shown in Fig. 8(a). Peak positions, indicated by arrows, shift backwards from $\eta = 1.51$ to 1.38, in going from the lighter to the heavier target. Although this shift is not large, it is in a region where the relative azimuthal coverage of the array [the shaded curve in Fig. 8(a)] is falling off. The acceptance of PbGl array, i.e., the ratio of the in-

tercepted transverse energy to that which would have been recorded by a detector having the same detection properties but with 4π coverage, is examined in detail in Fig. 8(b) for two classes of events. Acceptance is target independent for typical peripheral interactions (24 projectile spectators). For central events (no spectators), there is a $\sim 12\%$ decrease in going from Al to Au, a consequence of the backwards shift of the pseudorapidity distribution. The observed saturation of the upper edges of PbGl spectra has been interpreted [5–7] as indicating projectile stopping in central collisions with nuclei heavier than Cu. The present calculation suggests that such saturation is not primarily an artifact of changes in the PbGl acceptance in the E802 geometry. The acceptance for central collisions decreases by only $\sim 6\%$ in going from Cu to Au.

^a Now at Xon Tech, Inc., Van Nuys, CA 91406.

^b Now at Lawrence Livermore National Laboratory, Livermore, CA 94550.

^c Now at Lawrence Berkeley Laboratory, Berkeley, CA 94720.

^d Now at Hitachi, Ltd., Ibaraki-ken 316, Japan.

^e Now at Schlumberger Corp., Houston, TX 77210.

^f Now at Nippon Telegraph and Telephone Co. Tsuyama, Tsuyama, Okayama 708, Japan.

^g Now at Los Alamos National Laboratory, Los Alamos, NM 87545.

^h Now at Weizmann Institute of Science, Rehovot 76100, Israel.

ⁱ Now at Mitsubishi Electric Co., Hyogo 652, Japan.

^j Now at UC Irvine, Irvine, CA 92717.

^k Now at Bruker Medical Imaging, Inc., Lisle, IL 60532.

^l Now at Bell Telephone Laboratory, Naperville, IL 60566.

^m Now at Continuous Electron Beam Accelerator Facility, Newport News, VA 23606.

[1] Proceedings of the Third Nucleus-Nucleus Collisions, Saint Malo, France, edited by C. Détraz, C. Estève, C. Grégoire, D. Guerreau, and B. Tamain [Nucl. Phys. **A488**, 1 (1988)]; Proceedings of Quark Matter '87, Nordkirchen, W. Germany, edited by H. Satz, H. J. Specht, and R. Stock [Z. Phys. C **38**, (1988)].

[2] T. Abbott *et al.*, Nucl. Instrum. Methods **A290**, 41 (1990).

[3] T. Abbott *et al.*, Phys. Rev. Lett. **64**, 847 (1990).

[4] B. Nilsson-Almqvist and E. Stenlund, Comput. Phys. Commun. **43**, 387 (1987); B. Andersson, G. Gustafson, and B. Nilsson-Almqvist, Nucl. Phys. **B281**, 289 (1987).

[5] T. Abbott *et al.*, Phys. Lett. B **197**, 285 (1987).

[6] L. Remsberg *et al.*, Z. Phys. C **38**, 35 (1988).

[7] P. Braun-Munzinger *et al.*, Z. Phys. C **38**, 45 (1988).

[8] For a general review of transverse energy measurements, see, M. J. Tannenbaum, Int. J. Mod. Phys. A **4**, 3377 (1989).

[9] Y. Akiba, Ph.D. thesis, University of Tokyo, 1989.

[10] The symbols E_{TOT}^{PbGl} and E_T^{PbGl} used in the present work are identical with the E_{TOT}^0 and E_T^0 of earlier references. The favored superscript PbGl serves to emphasize that the PbGl array is sensitive to both charged and neutral particles.

[11] G. Young *et al.*, Nucl. Instrum. Methods **A279**, 503 (1989).

[12] D. Beavis *et al.*, Nucl. Instrum. Methods **A281**, 367 (1989).

[13] R. Albrecht *et al.*, Phys. Lett. B **199**, 297 (1987).

[14] W. Heck *et al.*, Z. Phys. C **38**, 19 (1988).

[15] D. E. Greiner, P. J. Lindstrom, H. H. Heckman, B. Cork, and F. S. Bieser, Phys. Rev. Lett. **35**, 152 (1975).

[16] M. I. Adamovich *et al.*, Phys. Rev. C **40**, 66 (1989).

[17] C. Brechtmann, W. Heinrich, and E. V. Benton, Phys. Rev. C **39**, 2222 (1989).

[18] A. Bialas, M. Bleszyński, and W. Czyż, Nucl. Phys. **B111**, 461 (1976).

[19] A. Bamberger *et al.*, Phys. Lett. B **184**, 271 (1987).

[20] J. Ftačnik, K. Kajantie, N. Pisutova, and J. Pisut, Phys. Lett. B **188**, 279 (1987).

[21] H. vonGersdorff *et al.*, Phys. Rev. C **39**, 1385 (1989).

[22] T. Abbott *et al.*, Phys. Rev. Lett. **66**, 1567 (1991).

[23] The present calculations used version 1.7 of this code with three parameters adjusted to fit experimental $p+p$ data at AGS energies. Adopted values of a , b , and σ were 1.0, 0.4, and 0.55, respectively; see J. B. Costales, Report E-802-MEM-8, 1988 (unpublished).

[24] A. VanGinneken and M. Awaschalom, Fermilab report, Batavia, IL, 1975; A. VanGinneken, Fermilab Report FN-272, Batavia, IL, 1975.

[25] This is a simple approximation to the complex response of the PbGl to charged particles. Other assumptions such as a gradual turn-on of Čerenkov light above the true threshold at $\beta = 0.6$ were explored and found not to change the conclusions significantly.